JMB

Identification of a Key Structural Element for Protein Folding Within β-Hairpin Turns

Jaewon Kim, Stephen R. Brych, Jihun Lee, Timothy M. Logan and Michael Blaber*

Kasha Institute of Molecular Biophysics and Department of Chemistry and Biochemistry Florida State University Tallahassee, FL 32306-3015 USA

Specific residues in a polypeptide may be key contributors to the stability and foldability of the unique native structure. Identification and prediction of such residues is, therefore, an important area of investigation in solving the protein folding problem. Atypical main-chain conformations can help identify strains within a folded protein, and by inference, positions where unique amino acids may have a naturally high frequency of occurrence due to favorable contributions to stability and folding. Non-Gly residues located near the left-handed α-helical region (L-α) of the Ramachandran plot are a potential indicator of structural strain. Although many investigators have studied mutations at such positions, no consistent energetic or kinetic contributions to stability or folding have been elucidated. Here we report a study of the effects of Gly, Ala and Asn substitutions found within the L-α region at a characteristic position in defined β-hairpin turns within human acidic fibroblast growth factor, and demonstrate consistent effects upon stability and folding kinetics. The thermodynamic and kinetic data are compared to available data for similar mutations in other proteins, with excellent agreement. The results have identified that Gly at the $i+3$ position within a subset of β-hairpin turns is a key contributor towards increasing the rate of folding to the native state of the polypeptide while leaving the rate of unfolding largely unchanged.

© 2003 Elsevier Science Ltd. All rights reserved

Keywords: β-hairpin; fibroblast growth factor; folding kinetics; stability; trefoil

Corresponding author

Introduction

Non-Gly residues located in the left-handed α-helical region (L-α) of the Ramachandran plot ($0° < \phi < +90°$, $0° < \psi < +90$) have attracted attention due to the potential for structural strain between side-chain C^β and main-chain groups.[1–7] Evaluation of strain has been experimentally quantified by comparing equivalent Gly and Ala mutations at these positions, however, no consistent contribution to the overall stability of the protein has been demonstrated. Likewise, no clear understanding has emerged of the contribution of such structural features to protein folding. Here we have focused upon the contribution to stability and folding of residues in the L-α position of the Ramachandran plot that are located at the $i+3$

position in type I β-hairpin turns of either the 3:5 or 4:6 type. Thornton and co-workers have developed the shorthand for β-hairpin structures, which communicates the relevant structural details for the different types.[8] In this shorthand an integer prefix identifies the number of residues required for the turn. This is followed by a colon and an integer suffix that identify the hydrogen bonding pattern in the closure of the turn (the general formula being that if two hydrogen bonds are formed at the closure, then the suffix = prefix; however, if only one hydrogen bond forms the closure, then the suffix = prefix + 2). Thus, a 2:2 β-hairpin has two residues in the turn and two hydrogen bonds in the turn closure. A 3:5 β-hairpin has three residues in the turn and a single hydrogen bond in the turn closure. The β-hairpin nomenclature does not provide information regarding the type of turn conformation within the turn region, as this is identified using the turn formalism of Richardson[9] (e.g. type I, II, I′, II′, etc.). A comprehensive analysis of protein structures

derived from X-ray data with resolution better than 2.5 Å (derived from CATH Sreps v2.4) identified 43,323 β turns of which 14,391 (33.2%) are type I. Of these 14,391 type I β-turns 11,863 occur as single turns, with the remainder forming part of two or more overlapping turns. Of these 14,391 single type I β turns, 1435 have the $i + 3$ residue in the left-handed α-helical conformation (9.97%) with 461 (32.9%) of these being Gly. This analysis indicates that there are more than 900 $i + 3$ non-Gly residues located in the L-α region (E. G. Hutchinson, personal communication).

Matthews and co-workers studied the effects of Gly substitutions at two positions (Asn55 and Lys124) in phage T4 lysozyme that are located in the L-α region of the Ramachandran plot.[1] Position 55 is located at the $i + 1$ position of a type I′ β-turn (not part of a β-hairpin) and residue position 124 is not part of any defined β-turn. A Gly mutation at position 55 was essentially identical in stability to the wild-type protein, whereas a Gly mutation at position 124 destabilized the protein by approximately 2.1 kJ/mol.

Nakamura and co-workers identified a stabilizing Gly mutation at position 95 in *Thermus thermophilus* ribonuclease HI in comparison to a Lys residue at the same position in *Escherichia coli* ribonuclease.[2] This residue is located at a surface-exposed $i + 3$ position in a type I 3:5 β-hairpin turn, and is located in the L-α region of the Ramachandran plot. A Gly mutation at this position resulted in the stabilization of the *E. coli* ribonuclease by 7.5 kJ/mol in comparison to Ala. Additionally, an Asn substitution at this position stabilized the protein by approximately 3.3 kJ/mol in comparison to Ala.

Stites and co-workers studied the effects of Gly and Ala mutations at residue positions in staphylococcal nuclease that exhibit atypical φ, ψ angles in the Ramachandran plot.[3] Among this set of residue positions are ten that occur in the L-α region. Two of the ten positions are located within type II turns, two are in type IV turns, two are in overlapping type I′ and type IV turns, one is in a type I turn and three are not within any defined turn type. Only two of the ten positions comprise β-hairpin turns and these are both type IV 2:2 "tight" β-hairpin turns. Ala → Gly mutations for the set of ten positions resulted in a wide range of effects upon stability, from 2.5 kJ/mol destabilizing to 18.4 kJ/mol stabilizing.[3]

Baker and co-workers have studied the effects upon stability, folding and domain swapping of Gly → Ala mutations within two β-hairpins in the B1 domain of Protein L from *Peptostreptococcus magnus*.[4,10] The first β-hairpin (residues 12–15) is classified as a type I 3:5 β-hairpin and contains a Gly residue at the $i + 3$ position that is located in the L-α region of the Ramachandran plot. The second β-hairpin (residues 52–55) is classified as a 4:4 β-hairpin but there is no defined β-turn type, and Zhang and co-workers describe it as a distorted type I′ turn.[4,10] Residues 53, 54 and 55 are in

the L-α region of the Ramachandran plot with residue $i + 3$ (position 55) a Gly in this turn also. Stability studies of Gly → Ala mutations indicate that an Ala mutation at position 15 destabilizes the protein by 6.7 kJ/mol, and an Ala mutation at position 55 destabilizes the protein by 8.8 kJ/mol. Kinetic studies of these mutations indicate that the type I 3:5 β-hairpin (residues 12–15) is formed at the folding transition state, while the 4:4 β-hairpin (residues 52–55) is not. Furthermore, the Ala mutation at position 15 decreased the folding rate, but had little effect upon the unfolding rate. In contrast, the Ala mutation at position 55 increased the unfolding rate and had minimal effect upon the folding rate.[4]

Frieden and co-workers reported a study of "turn-scanning" mutations in nine different turn regions between β-strands of Intestinal Fatty Acid Binding Protein (IFABP).[5] These turns included three type II′, two type I, one each of type I′, II, and IV, and one undefined turn type. One of the type I turns comprised a 4:6 β-hairpin with the $i + 3$ residue in the L-α region of the Ramachandran plot. Although no Ala mutations were studied, conversion of the $i + 3$ positions within each of these turns to Val resulted in a range of effects upon stability, varying from 2.3 kJ/mol destabilizing to 9.6 kJ/mol stabilizing. The substitution of the wild-type $i + 3$ Gly residue in the type I 4:6 β-hairpin ($i + 3$ L-α) to a Val destabilized the protein by 10.5 kJ/mol.[5]

Ueda and co-workers studied a series of Ala mutations at five positions within hen egg white lysozyme that were Gly in the wild-type structure, located in the L-α region of the Ramachandran plot, and on the surface of the structure.[6] Two of these positions were the $i + 1$ residue in a type IV turn, two were the $i + 2$ residue in a type II turn and one was the $i + 3$ residue in a type I 3:5 β-hairpin turn (the only β-hairpin example in the study). Gly → Ala mutations at these positions resulted in a diverse set of effects upon stability, ranging from 0.1 kJ/mol stabilizing to 7.9 kJ/mol destabilizing.

Yutani and co-workers constructed a series of Gly and Ala substitutions at six different residue positions in human lysozyme that are located within the L-α region of the Ramachandran plot.[11] Three of the six positions are located in a type I turn, one is within a type I′ turn, one is in a type IV turn and the other position is not located in an identifiable turn type. Of the three type I turns, two are type 4:4 β-hairpins and the other is not a β-hairpin type turn. Of the two type I 4:4 β-hairpins one is almost completely solvent-inaccessible (Gln58) and the other partially accessible (Arg50). $\Delta\Delta G$ values for corresponding Ala → Gly substitutions at these two positions indicated that a Gly substitution at position 50 destabilized the structure by 0.7 kJ/mol, whereas a Gly substitution at position 58 stabilized the structure by 4.0 kJ/mol.[11] The remaining positions studied either stabilized or destabilized the structure over a range of 1.4 kJ/mol. This group reported an additional
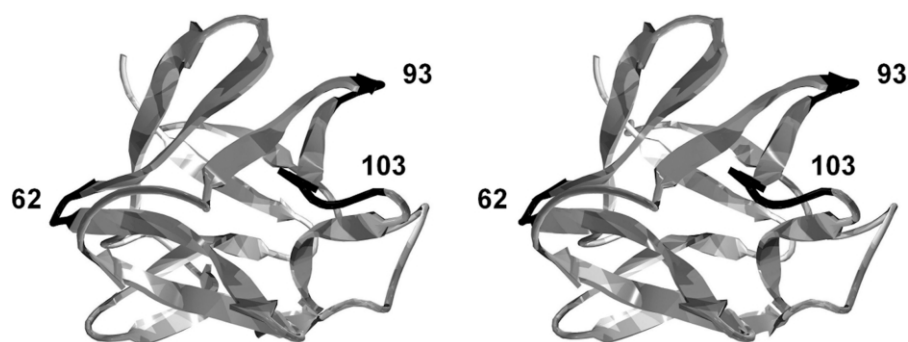
Figure 1. Ribbon diagram of FGF-1,[12] the view is approximately normal to the 3-fold axis of the β-barrel. Also indicated are the locations of β-hairpin turns at positions 62, 93 and 103.

study of ten Gly → Ala substitutions in human lysozyme of which six were located within the L-α region of the Ramachandran plot.[7] Of these six positions, one is located at the $i + 1$ position of a type I′ turn, two are located at the $i + 2$ position of a type II turn, and three are not within an identifiable turn type. None of the type I′ or II turns are β-hairpin turns. The effects of an introduced Ala side-chain at these positions generally destabilized the protein, with $\Delta\Delta G$ values ranging from 1.2 kJ/mol to 7.5 kJ/mol, however, one Ala mutation resulted in an increase in stability of 0.6 kJ/mol.[7]

The above studies highlight the difficulty in predicting the contribution to protein stability of residues located within the L-α region of the Ramachandran plot, and indicate that other structural determinants must be considered in order to understand the effects upon stability and folding.

The model system employed here is human acidic fibroblast growth factor (FGF-1)†, whose thermodynamic and structural properties have been described.[12,13] FGF-1 is a member of a family of heparin-binding mitogens and hormones[14,15] and exhibits a β-trefoil structure, one of the fundamental protein superfolds.[16] This fold contains six two-stranded β-hairpins (for a total of 12 β-strands), three that form an "upper" β-barrel structure and three that form a "lower" β-hairpin triplet, or triangular array, that caps the barrel at one end[17] (Figure 1). The β-barrel region is involved mainly in binding to FGF receptors and the triangular array contains a heparin binding region.[12,18–23] The arrangement of the secondary structure gives FGF-1 a pseudo 3-fold internal symmetry. There are 11 turn regions in FGF-1 and nine of them are defined as type I β turns (Figure 2).

We have been able to identify a consistent effect of Ala → Gly substitutions upon the stability and folding kinetics for positions located with the L-α region of the Ramachandran plot and within a type I β-turn. Furthermore, we have extended the stability studies to include an analysis of the contribution of these positions towards folding and unfolding kinetic constants and the transition state (ϕ value). The kinetic data show that Gly residues at these positions are key residues contributing to the "foldability" of the polypeptide, and ϕ_{unf} value analysis indicates that these positions are essentially as structured in the folding transition state as they are in the native state. We have tested the predictability of the thermodynamic and kinetic effects of a Gly residue at the $i + 3$ position in a type I β-hairpin turn by engineering such a turn into the structure of FGF-1, and these results are in close agreement with the data from the other turns.

Results

Each mutant protein expressed at a level typical of the recombinant wild-type protein (approximately 50–100 mg/l) and exhibited characteristic chromatographic profiles during purification. No unusual aggregation or precipitation properties were observed for any of the mutant proteins.

The results of the isothermal equilibrium denaturation analysis are listed in Table 1. We have previously reported a comprehensive stability study of wild-type (non-His-tagged) FGF-1 utilizing both differential scanning calorimetry (DSC) and isothermal equilibrium denaturation monitored by
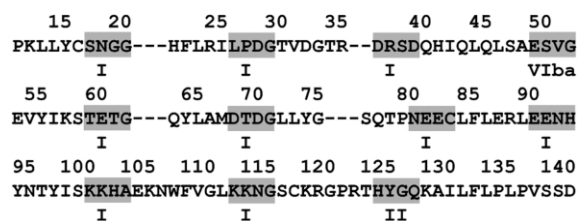
Figure 2. Primary sequence alignment of FGF-1 to indicate the internal 3-fold symmetry characteristic of the β-trefoil fold. Also indicated are the locations and types of identified β-turns. For each turn the shaded region identifies the i through $i + 3$ position within the turn.

Table 1. Thermodynamic parameters for WT FGF-1 and mutant proteins determined from isothermal equilibrium denaturation

Protein	ΔG_0 (kJ/mol)	m-value (kJ/mol M)	C_m (M)	$\Delta\Delta G^a$ (kJ/mol)
WT	21.1 ± 0.6	-18.9 ± 0.6	1.11 ± 0.01	–
Asn106 → Gly	22.7 ± 0.5	-20.7 ± 0.9	1.10 ± 0.02	0.2
His93 → Gly	28.6 ± 0.1	-19.8 ± 0.1	1.45 ± 0.01	$-6.6 \; (-9.7)^b$
His93 → Ala	19.3 ± 0.1	-20.4 ± 0.3	0.95 ± 0.02	3.1
His93 → Asn	22.3 ± 0.3	-19.8 ± 0.1	1.13 ± 0.02	-0.4
Gly62 → Ala	15.1 ± 0.7	-19.2 ± 0.9	0.79 ± 0.01	6.1
Gly62 → Asn	17.8 ± 0.6	-20.5 ± 0.8	0.87 ± 0.01	4.7
Ala103 → Gly	19.4 ± 0.6	-19.4 ± 0.3	1.00 ± 0.01	2.1
ΔEKN	22.0 ± 0.4	-18.6 ± 0.4	1.19 ± 0.01	-1.5
ΔEKN/Ala103 → Gly	26.8 ± 0.8	-17.9 ± 0.6	1.49 ± 0.01	$-7.0 \; (-5.5)^c$
ΔEKN/Ala103 → Asn	24.5 ± 0.5	-19.0 ± 0.7	1.29 ± 0.02	$-3.4 \; (-1.9)^c$

    [a] $\Delta\Delta G = (C_{m \text{ wild-type}} - C_{m \text{ mutant}})(m_{\text{wild-type}} + m_{\text{mutant}})/2.$[31] A negative value for $\Delta\Delta G$ indicates a more stable mutant.
    [b] Values in parentheses are in relationship to the His93 → Ala mutant.
    [c] Values in parentheses are in relationship to the ΔEKN mutant. All errors are listed as standard error of multiple data sets.

both fluorescence and circular dichroism spectroscopy.[13] This study demonstrated excellent cross-validation of the ΔG_u values determined using these different methods and a two-state assumption. Analysis of the isothermal equilibrium data for the His-tagged wild-type protein yields a ΔG_0 value of 21.1 kJ/mol, with an m value of -18.9 kJ/mol M and a C_m value of 1.11 M (Table 1). This compares favorably with the values previously reported for the non-His-tagged wild-type protein of $\Delta G_0 = 21.3$ kJ/mol, m value $= -18.8$ kJ/mol M and $C_m = 1.13$ M.[13] An overlay of the ΔG_u *versus* denaturant concentration data for isothermal equilibrium denaturation of both wild-type and His-tagged wild-type FGF-1 is essentially indistinguishable (data not shown). We conclude, therefore, that the addition of the amino-terminal His-tag has had no discernable effect upon the thermodynamic properties of FGF-1.

The results of the folding and unfolding kinetic analysis are listed in Table 2. The unfolding kinetic data, in every case, exhibited an excellent fit to a single exponential decay model. The folding kinetic data also exhibited an excellent fit to a single exponential decay model, but only for concentrations of denaturant greater than approximately 0.6 M. At denaturant concentrations below this critical level, a bi-exponential decay model fit the data with acceptable values for the residuals. The fast phase of this bi-exponential region of folding followed the linear trend of $\ln(k_f)$ *versus* denaturant concentration characteristic of the single exponential region of folding. A predicted folding rate constant function was generated using the K_{eq} values from the isothermal equilibrium denaturation data in conjunction with the unfolding rate constant data. In all cases, this predicted function followed closely the fast phase of the bi-exponential region (data not shown). In contrast, folding rate constants within the slow phase of the bi-exponential region were generally independent of denaturant concentration, and describe a "roll-over" region in the chevron plot (Figure 3). The above-described features of the folding of FGF-1 are shared by all other members of the β-trefoil family, including FGF-2 (basic FGF),[24] interleukin-1β[25,26] and hisactophilin[27] and have also been described for FGF-1 with urea

Table 2. Folding and unfolding kinetic parameters, and derived thermodynamic parameters, for WT FGF-1 and mutant proteins

Protein	k_f (s^{-1})	m_f (M^{-1})	k_u (1×10^{-3} s^{-1})	m_u (M^{-1})	ϕ_{unf}	$\Delta\Delta G^a$ (kJ/mol)
WT	3.74	-6.61	0.808	0.46	–	–
Asn106 → Gly	3.65	-6.40	0.850	0.49	0.63	-0.4
His93 → Gly	55.05	-7.43	0.439	0.47	$0.19 \; (0.21)^b$	$-5.4 \; (-8.9)^b$
His93 → Ala	2.43	-7.19	1.170	0.42	0.29	3.5
His93 → Asn	5.95	-6.86	0.716	0.48	0.77	-0.6
Gly62 → Ala	0.96	-7.55	0.820	0.48	0.01	5.9
Gly62 → Asn	1.67	-7.50	0.999	0.45	0.11	4.8
Ala103 → Gly	2.21	-5.82	1.720	0.46	0.89	0.9
ΔEKN	3.16	-5.73	0.811	0.70	–	-1.6
ΔEKN/Ala103 → Gly	13.63	-5.31	0.522	0.70	$(0.20)^c$	$-8.1 \; (-6.5)^c$
ΔEKN/Ala103 → Asn	4.88	-5.88	0.474	0.66	$(0.71)^c$	$-3.8 \; (-2.2)^c$

    [a] $\Delta\Delta G = (C_{m \text{ wild-type}} - C_{m \text{ mutant}})(m_{\text{wild-type}} + m_{\text{mutant}})/2,$[31] where all parameters are derived from the kinetic data. A negative value for $\Delta\Delta G$ indicates a more stable mutant.
    [b] Values in parentheses are calculated in relationship to the His93 → Ala mutant.
    [c] Values in parentheses are calculated in relationship to the ΔEKN mutant.
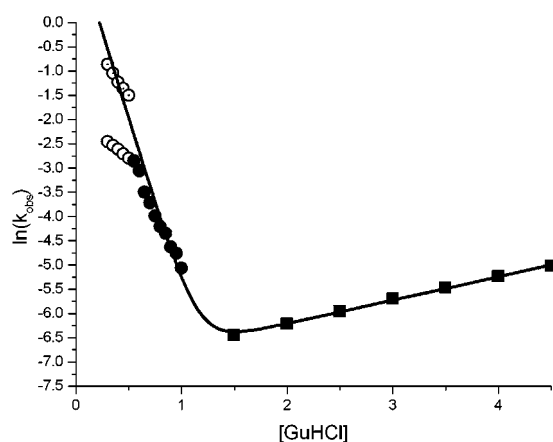
Figure 3. Folding (filled circles) and unfolding (filled squares) kinetic data for wild-type FGF-1 in guanidine hydrochloride denaturant. The slow phase of the bi-exponential region of the folding is indicated by the open circles, and the fast phase by the circles with a central dot. The fit shown was determined from the isothermal equilibrium data and the unfolding kinetic data and indicates the predicted folding kinetic behavior assuming a two-state model.

denaturant.[28] The folding and unfolding rate constants for each mutant listed in Table 2 were therefore determined using the entire unfolding data, in combination with the single exponential region of folding, and the fast phase of the bi-exponential region of folding, as a global fit. Folding involving dilution into the lowest concentrations of denaturant in the study (i.e. 0.25 M GuHCl) exhibited a transient increase in the fluorescence signal, detectable within the first 150 ms (Figure 4). This initial region of the folding data was therefore omitted prior to model fitting.

The folding and unfolding kinetic data permit a calculation of the expected equilibrium constant for unfolding as a function of denaturant, and
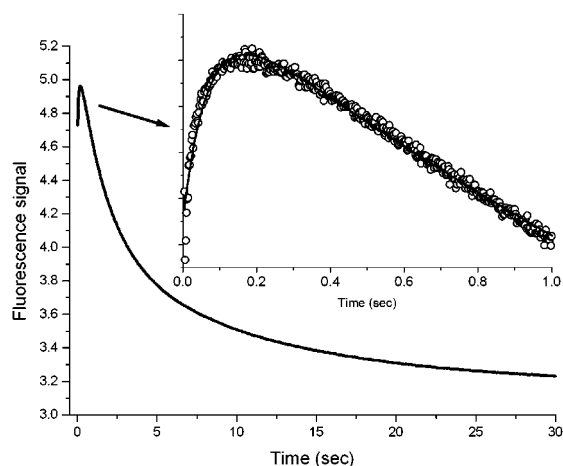
Figure 4. Folding kinetic data for FGF-1 into 0.25 M guanidine hydrochloride denaturant indicating an initial increase in fluorescence ($\tau = 66$ ms) of Trp107 due to desolvation (see the text).
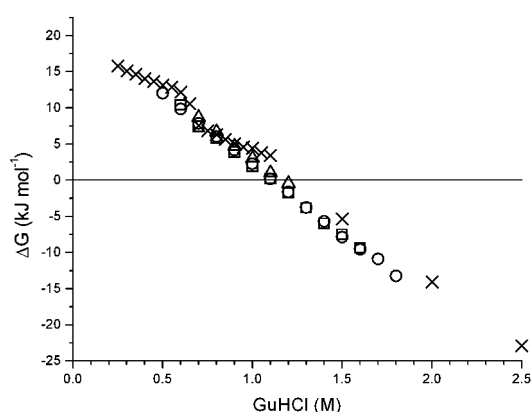
Figure 5. ΔG_u values for wild-type FGF-1 at 298 K using guanidine hydrochloride as denaturant as determined by isothermal equilibrium denaturation monitored by fluorescence (circles), kinetics monitored by fluorescence (crosses), isothermal equilibrium denaturation monitored by circular dichroism (squares)[13] and differential scanning calorimetry (up triangles).[13]

therefore, the value of ΔG_u as a function of denaturant. The $\Delta\Delta G_u$ values for the mutations can likewise be determined in comparison to the wild-type or other reference mutant. The $\Delta\Delta G_u$ values, generated from the kinetic data, are listed in Table 2 and can be compared to the $\Delta\Delta G_u$ values derived from the isothermal equilibrium denaturation data in Table 1. The standard deviation for the agreement between the two sets of $\Delta\Delta G_u$ values is 0.5 kJ/mol, or similar to the deviation of the values of ΔG_0 determined by isothermal equilibrium denaturation (Table 1) and to the deviation observed when comparing ΔG_0 values determined by DSC and isothermal equilibrium experiments.[13] Thus, the isothermal equilibrium and kinetic measurements are in good agreement (Figure 5), and 0.5 kJ/mol is taken to be the standard deviation of ΔG_u determinations regardless of method. Given that the unfolding kinetic data follow a simple exponential decay model in each case, determination of ϕ_{unf} is expected to be a more accurate metric of mutational effects upon the transition state energy than ϕ_f.[29] If $\phi_{unf} = 1.0$ then $\Delta G_\ddagger = \Delta G_U$ and the region of the mutation is as unfolded in the transition state as in the unfolded state, likewise, if $\phi_{unf} = 0$ then $\Delta G_\ddagger = \Delta G_F$ and the region of the mutation is as folded in the transition state as in the native state.[29] The ϕ_{unf} values for the various mutations are listed in Table 2.

Discussion

In a previous study[13] we have shown that FGF-1 undergoes two-state reversible thermal denaturation in the presence of a critical concentration (i.e. >0.6 M) of added GuHCl. Below this concentration, the thermal denaturation does not fit a two-state model and thermally induced aggregation

can occur with lower denaturant concentrations. The present kinetic study supports these prior results and demonstrates that at [GuHCl] < 0.6 M the folding of FGF-1 exhibits a fast and slow phase. The slow folding phase relaxation time of 10.4 seconds is independent of the introduced mutations and therefore suggests a shared physical basis. The slow folding phase below a critical denaturant concentration is observed in all members of the β-trefoil family of proteins that have been characterized to date, including FGF-1,[28] FGF-2 (basic FGF),[24] interleukin-1β[25,26] and hisactophilin.[27] However, the nature of the slow folding phase in this family of proteins (the β-trefoils) is a matter of some debate. Yu and co-workers have proposed that the slow refolding phase in FGF-1 is consistent with Pro isomerization.[28] However, Estape & Rinas have argued that the low activation enthalpy of refolding observed for the slow folding phase of FGF-2 is inconsistent with Pro isomerization.[24] Furthermore, hisactophilin exhibits the slow folding phase, however, its primary sequence is devoid of Pro residues.[27] Quenched-flow deuterium/hydrogen exchange experiments have identified secondary structure elements that form early and late in the folding pathway for the various β-trefoil proteins, however, these results demonstrate that there is no conserved folding pathway. For example, the earliest folding event in FGF-1 is the β-sheet formation between the amino and carboxyl termini (β-strands I and XII), with the slowest folding events involving strands II, III, VI–VIII and XII.[28] The earliest folding event in interleukin-1β involves strands VI–X, with the slowest involving strands I–III, V and XI.[25] In histactophilin strands IV–VIII fold first, while strands I–III and X–XII fold last.[27] With regard to the slow folding phase rate constants, hisactophilin appears to be the fastest ($k_{slow} \sim 1.0 \text{ s}^{-1}$), with FGF-1 intermediate in rate ($k_{slow} \sim 0.1 \text{ s}^{-1}$) and interleukin-1β the slowest ($k_{slow} \sim 0.03 \text{ s}^{-1}$). We note that there is a general relationship between these rates and the compactness or proximity within the native structure of the slowest folding regions (e.g. hisactophilin exhibits the fastest kinetics for the slow refolding phase and strands I–III and X–XII form a contiguous region in the native structure). The nature of the slow folding phase remains a matter for further investigation.

Here we were able to identify an increase in fluorescence signal within the first 150 ms of folding. Trp107 is buried in the native state and is more efficiently quenched than in the denatured state. This residue in the native state packs against His102 and Pro121[12] and these interactions contribute to the efficient quenching in the native state. Thus, the atypical quenching of Trp107 requires formation of a native-like assembly of residues 102, 107 and 121. In the denatured state Trp107 is solvent-exposed, and although not as efficiently quenched as in the native state, is still quenched to a certain extent by solvent. It is reasonable to

assume that during the folding of FGF-1 Trp107 must initially desolvate prior to formation of buried native-like interactions between His102 and Pro121. Thus, the increase in the fluorescence signal observed in the first 150 ms ($\tau = 66$ ms) is consistent with an "on pathway" initial desolvation event for Trp107 rather than representing an "off-pathway" burst phase. Observation of this initial desolvation event of Trp107 in the folding of FGF-1, and determination of the associated relaxation time, has not been described.

Folding and unfolding kinetics of L-α region Gly residues at the $i + 3$ position in type I 3:5 β-hairpin turns

We have previously reported a Gly scanning stability study of the turn region comprising residues 91–93 in FGF-1.[30] This turn is a type I 3:5 β-hairpin turn[8,9] in the FGF-1 structure where the $i + 3$ residue (position 93) is located in the L-α region of the Ramachandran plot. X-ray structure and stability studies demonstrated that a Gly residue at the $i + 3$ position stabilized the protein by elimination of steric interactions between the side-chain C^β and main-chain atoms in the native structure.[30] The kinetic data here show that the basis of the 9.7 kJ/mol increase in stability for an Ala → Gly mutation at position 93 is due to an approximately 23-fold increase in the rate of folding, with only a 2.7-fold increase in the rate of unfolding (Table 2, Figure 6). Positions 62 and 106 provide relevant comparisons to position 93. In the case of residue 62, the wild-type Gly is located at the $i + 3$ position in a type I 4:6 β-hairpin and is located in the L-α region of the Ramachandran plot. The kinetic data show that the basis of the 6.1 kJ/mol increase in stability for an equivalent Ala → Gly mutation at this position is due to an approximately fourfold increase in the rate of folding, and essentially no change in the rate of unfolding (Table 2, Figure 6). Residue Asn106 is likewise located in the L-α region, however, it is not part of a β-hairpin turn and is not within an identifiable turn type. There is essentially no change in the stability for an equivalent Ala → Gly mutation at this position, and both the folding and unfolding kinetic constants remain unchanged (Table 2, Figure 6). Baker and co-workers have reported thermodynamic and kinetic parameters comparing Ala and Gly residues at position 15 in peptostreptococcal Protein L.[4] This residue is also located at the $i + 3$ position in a type I 3:5 β-hairpin and is in the L-α region. An equivalent Ala → Gly mutation at this position stabilizes the protein by 6.7 kJ/mol and is due to an 8.5-fold increase in the rate of folding with only a 1.4-fold increase in the rate of unfolding.[4] Nakamura and co-workers reported stability studies for an equivalent Ala → Gly mutation at position 95 in ribonuclease HI. This residue is also located at the $i + 3$ position in a type I 3:5 β-hairpin and is in the L-α region. This group reported an increase in stability of
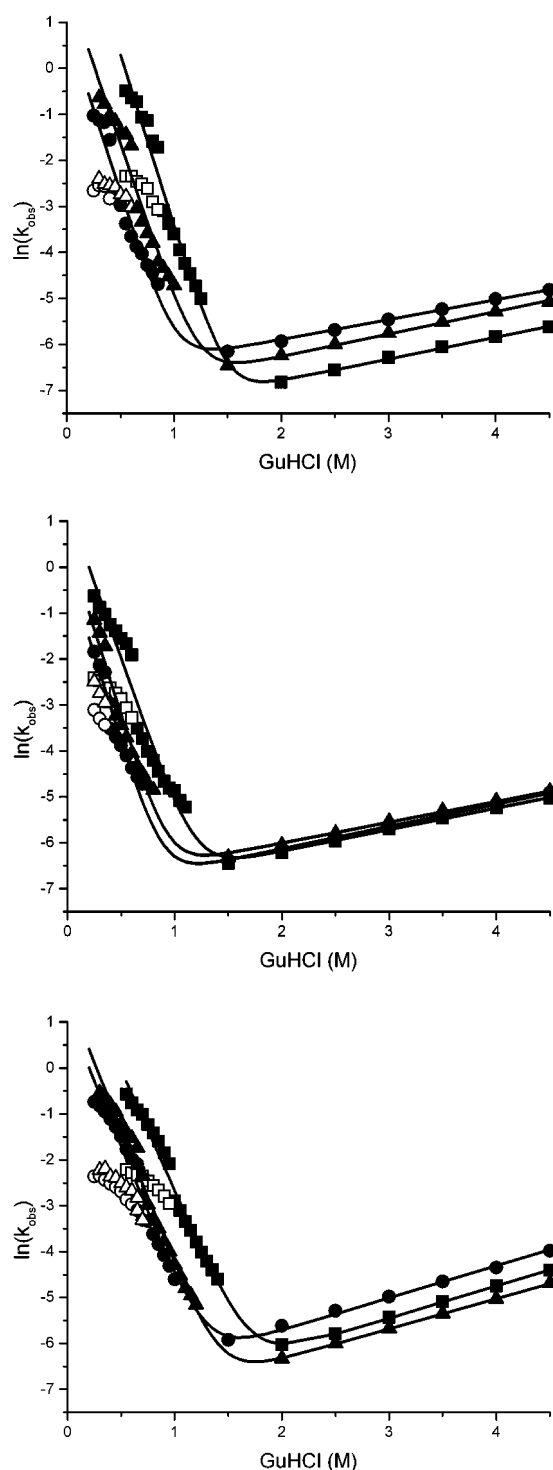
Figure 6. Folding and unfolding kinetic data and chevron plot global fit for Ala (circles), Asn (triangles) and Gly (squares) at positions 93 (top panel), 62 (middle panel) and 103 (in ΔEKN background; lower panel). The slow phase of the bi-exponential region of refolding is indicated by the open symbols.

7.5 kJ/mol for an Ala → Gly mutation at this position, although no kinetic data was determined. Udea and co-workers determined the effect upon stability for a Gly → Ala mutation at position 49 in hen egg white lysozyme.[6] This residue is likewise

the $i + 3$ position in a type I 3:5 β-hairpin turn. The $\Delta\Delta G$ value for the equivalent Ala → Gly mutation at this position was reported to be 7.9 kJ/mol. The thermodynamic and kinetic properties of Ala → Gly mutations at each of these structurally equivalent positions are remarkably consistent (Table 3) despite the fact that they occur within distinctly different protein folds. Although ϕ_{unf} values can be directly compared only for the Protein L and FGF-1 studies, they are quite similar (0.1 and 0.2, respectively) and indicate that in both cases the site of mutation is largely in the native conformation in the folding transition state. Although a ϕ_{unf} value was not reported for the ribonuclease HI study, the similar effects of the Ala → Gly mutation upon the folding and unfolding kinetics suggests that it would have a similar ϕ_{unf} value. It is also important to note that the local sequences within each of these type I 3:5 β-hairpin turns is different, with the exception of a conserved Asx residue at the $i + 2$ position (Table 3). While the thermodynamic and kinetic features of the above four sites are remarkably similar, they are substantially different from the Ala → Gly mutation at position 106 in FGF-1 (Tables 1 and 2), which shares no other structural feature other than a similar location in the Ramachandran plot.

Folding and unfolding kinetics of L-α region Gly residues at the $i + 3$ position in type I 4:6 β-hairpin turns

We also studied an Ala → Gly mutation at position 62 in FGF-1, which is the $i + 3$ position in a type I 4:6 β-hairpin, and is located in the L-α region of the Ramachandran plot. The effects upon stability, folding and unfolding rates for an Ala → Gly mutation at this position have already been discussed. The ϕ_{unf} value analysis for this mutation also indicates that this position is in the native conformation in the folding transition state (Table 3). Frieden & Kim reported thermodynamic and kinetic results for a Gly → Val substitution in IFABP at position 99, which is also the $i + 3$ position in a type I 4:6 β-hairpin, and is located in the L-α region of the Ramachandran plot.[5] An equivalent Val → Gly substitution at this position stabilizes the protein by 10.5 kJ/mol. However, this is the extrapolated value at 0 M denaturant and the wild-type and mutant proteins have significantly different m values,[5] therefore, we have recalculated the value of $\Delta\Delta G$ as 7.5 kJ/mol using the method of Pace[31] (Table 3). Although Frieden & Kim did not report a ϕ_{unf} value and k_u for this mutant, the value of k_f was reported and indicates that the equivalent Val → Gly substitution resulted in a 45-fold increase in the rate of folding. Thus, the primary effect of the mutation appears to be on k_f.

FGF-1 exhibits an internal 3-fold symmetry characteristic of the β-trefoil family of proteins.[17] Residue Ala103 is related to Gly62 by this internal

Table 3. Comparison of thermodynamic and kinetic parameters for Ala → Gly mutations at the $i + 3$ position within type I 3:5 and 4:6 β-hairpin turns

Protein	Turn seq.				Turn type	$i + 3$ Ala → Gly $\Delta\Delta G$ (kJ/mol)	$i + 3$ Ala → Gly ϕ_{unf}
FGF-1	90 Glu	91 Glu	92 Asn	93 His	Type I 3:5 β-hairpin $i + 3$ in L-α	−9.7	0.2
Protein L B1 domain[a]	12 Phe	13 Ala	14 Asn	15 Gly	Type I 3:5 β-hairpin $i + 3$ in L-α	−6.7	0.1
Ribonuclease HI[b]	92 Thr	93 Ala	94 Asp	95 Lys	Type I 3:5 β-hairpin $i + 3$ in L-α	−7.5	–
Hen egg white lysozyme[c]	46 Asn	47 Thr	48 Asp	49 Gly	Type I 3:5 β-hairpin $i + 3$ in L-α	−7.9	–
FGF-1	59 Thr	60 Glu	61 Thr	62 Glu	Type I 4:6 β-hairpin $i + 3$ in L-α	−6.1	0.01
Intestinal fatty acid binding protein[d]	96 Val	97 Asp	98 Asn	99 Gly	Type I 4:6 β-hairpin $i + 3$ in L-α	−7.5[e] (Val → Gly)	-
FGF-1 Δ(EKN)	100 Lys	101 Lys	102 His	103 Ala	Type I 4:6 β-hairpin $i + 3$ in L-α	−5.5	0.2

[a] Refs. 4,10.
[b] Ref. 2.
[c] Ref. 6.
[d] Ref. 5.
[e] Calculated using the method of Pace[31] and the data reported by Kim & Frieden.[5]

symmetry (Figure 2). However, although region 100–103 is identified as a type I turn, it does not adopt a defined β-hairpin in the wild-type structure. In comparison to the symmetry-related positions, there appears to be a three-amino acid residue insertion after position 103 (Figure 2). We postulated that region 100–103 may not adopt the characteristic type I 4:6 β-hairpin due to this three-amino acid residue insertion. A deletion mutation (ΔEKN) was constructed to remove these three amino acid residues (residues 104–106). An Ala → Gly mutation at position 103 in the wild-type structure destabilizes the structure by 2.1 kJ/mol, and this is due to a 1.7-fold decrease in the rate of folding and a 2.1 increase in the rate of unfolding (Table 2). The ϕ_{unf} value for the Ala → Gly mutation at position 103 in the wild-type structure is 0.89, indicating that the site is essentially as unfolded in the transition state as it is in the denatured state. However, in the ΔEKN deletion mutation an Ala → Gly mutation now stabilizes the structure by 5.5 kJ/mol. This stabilization is due to a 4.3-fold increase in the rate of folding and only a 1.5-fold decrease in the rate of unfolding. Furthermore, the ϕ_{unf} value for the Ala → Gly mutation at position 103 in the ΔEKN deletion mutation has now shifted to a value of 0.20, indicating that this site is essentially as structured in the native state as it is in the transition state (Table 2). These results are consistent with the expected formation of a type I 4:6 β-hairpin due to this three-amino acid residue deletion. The two type I 4:6 β-hairpin structures studied, and the results reported by Kim & Friedman,[5] thus yield consist-

ent results for thermodynamic and kinetic effects associated with Gly → Ala mutations. Furthermore, the relative $\Delta\Delta G$ values and effects upon k_f and ϕ_{unf} values are consistent between the type I 3:5 and type I 4:6 β-hairpin structures (Table 3). As with the type I 3:5 β-hairpin turns, the amino acid sequences and protein folds are quite different and the thermodynamic and kinetic effects appear to be a consequence primarily of the conformation.

Yutani and co-workers have reported thermodynamic parameters for Gly → Ala substitutions in human lysozyme at the $i + 3$ position in type I 4:4 β-hairpin turns, with the $i + 3$ position in the L-α region.[11] The $\Delta\Delta G$ values for these mutations are 4.0 kJ/mol stabilizing (position 58) and −0.7 kJ/mol destabilizing (position 50) (Table 3). While the position 58 results are similar to the results observed here for 3:5 and 4:6 β-hairpin turns, the position 50 results are inconsistent. It may be that the type I 4:4 β-hairpin turns do not exhibit the same thermodynamic and kinetic properties as the 3:5 and 4:6 β-hairpin turns, or that there is some other structural feature affecting the position 50 results. In FGF-1 we have previously reported that the turn involving residue position 93 can adopt either a type I or type I′ configuration depending upon crystallization conditions (i.e. different space groups). Gly scanning mutagenesis identified the type I turn as most likely to be populated in solution.[30] We have crystallized FGF-1 in five different space groups $P2_1$ (two molecules/asu), $P2_1$ (three molecules/asu), $P2_12_12_1$, $C2$ and $C222_1$.[32] In each case, the structural features (turn types) involving residue positions

62, 103 and 106 are identical. Thus, there is no ambiguity in the assignment of the turn types for the positions studied in FGF-1. Furthermore, due to the nature of strand register in β-sheet structures it would require dramatic structural rearrangements (i.e. inversion of core-packing and surface residues) for 3:5 turns to convert to either tight 2:2 type hairpins or 4:6 turns (and *vice versa*).

Folding and unfolding kinetics of L-α region Asn mutations

As part of the present study we have included a series of Asn mutations at position 62, 93 and 103 (in the ΔEKN background). Asx residues are known to adopt conformations in the L-α region of the Ramachandran plot more readily than any other amino acid beside Gly.[33,34] Blundell and co-workers have determined that the side-chain carbonyl of 80% of such residues is frequently within 4 Å of their backbone carbonyl, or the backbone carbonyl of the preceding residue.[35] This carbonyl–carbonyl interaction provides an energetic rationale for the frequency of Asx residues observed in the L-α region. A comparison of equivalent Ala → Asn mutations at the position studies in FGF-1 indicates that this mutation can stabilize the structure by 1.4 kJ/mol (position 62), 3.5 kJ/mol (position 93) and 3.4 kJ/mol (position 103 in the ΔEKN mutant). These values agree well with the 3.3 kJ/mol increase in stability reported by Nakamura and co-workers for an equivalent Ala → Asn mutation at residue 95 in ribonuclease HI (also an $i + 3$ position in a type I 3:5 β-hairpin).[2] These results support the hypothesized stabilizing carbonyl–carbonyl interaction proposed for Asx residues in the L-α region and suggest an average stabilizing energy of approximately 3.0 kJ/mol. This stabilization arises from the favorable interaction between the partial positive charge on the carbon–oxygen dipole of one carbonyl with the partial negative charge on the oxygen–carbon dipole of the neighboring carbonyl.

These results show that the effects upon protein stability and folding for residue positions in the L-α of the Ramachandran plot can only be accurately understood with the inclusion of additional structural information. In particular, a consistent pattern of thermodynamic and kinetic properties are obtained for these residues if they are at characteristic $i + 3$ positions in type I 3:5, or 4:6, β-hairpin turns. In this regard, the role of Gly is to permit faster folding but to leave the rate of unfolding largely unaffected.

Materials and Methods

Mutagenesis and expression

All studies utilized a synthetic gene for the 140 amino acid residue form of human FGF-1[12,36–38] with the addition of an amino-terminal six His tag to facilitate purification.[32] The QuikChange™ site-directed mutagenesis protocol (Stratagene, La Jolla, CA) was used to introduce all point mutations, and all mutations were confirmed by nucleic acid sequence analysis (Biomolecular Analysis Synthesis and Sequencing Laboratory, Florida State University). All expression and purification followed previously published procedures.[32] Purified protein was exchanged into 20 mM *N*-(2-acetamido)-iminodiacetic acid (ADA), 100 mM NaCl, 2 mM DTT (pH 6.60) (ADA buffer) for biophysical studies.

Isothermal equilibration denaturation

Protein samples (40 to 10 μM) in various concentrations of GuHCl/ADA buffer were allowed to equilibrate overnight at room temperature (298 K). This study makes use of the fluorescence signal of the single endogenous Trp residue at position 107. This residue is ∼90% buried in the native structure.[12] Complete details of the instrumentation, data collection and analysis procedure have been reported.[13] Briefly, the fluorescence signal of FGF-1 is atypical in that Trp107 exhibits greater quenching in the native state rather than the denatured state. Excitation at 295 nm provides selective excitation of Trp107 in comparison with the six Tyr residues that are present in the structure.[13,32] Triplicate scans were collected and averaged. Buffer traces were collected and subsequently subtracted from protein scans. All scans were integrated to quantify the total fluorescence as a function of denaturant concentration. The data were analyzed using a general purpose non-linear least-squares fitting program (DataFit, Oakdale Engineering, Oakdale PA) implementing a six-parameter, two-state model:[39]

$$F = \frac{F_{0N} + S_N[D] + (F_{0D} + S_D[D])\, e^{-((\Delta G_0 + (m[D])/RT)}}{1 + e^{-((\Delta G_0 + m[D])/RT)}} \quad (1)$$

where the denaturant concentration is given by [D], the native state (0 M denaturant) fluorescence intercept and slope are F_{0N} and S_N, respectively, the denatured state fluorescence intercept and slope are F_{0D} and S_D, respectively, and the free energy of unfolding function intercept and slope are ΔG_0 and m, respectively. The ΔG_0 and m values describe the linear function of the free energy of unfolding as a function of denaturant under isothermal equilibrium conditions. The midpoint of the transition, i.e. the denaturant concentration where $\Delta G = 0$, is defined as C_m. The effect of a given mutation upon the stability of the protein ($\Delta \Delta G$) was calculated by taking the difference between the C_m values for wild-type and mutant and multiplying by the average of the m values, as described by Pace.[31]

Unfolding kinetic measurements

Prior to analysis native protein samples were dialyzed against 20 mM ADA 100 mM NaCl, 2 mM DTT (pH 6.60) overnight at 298 K. Unfolding was initiated by a 1:10 dilution of 25 μM protein into 20 mM ADA, 100 mM NaCl (pH 6.60) with concentrations of GuHCl between 1.5 M to 5 M. The fluorescence signal associated with protein unfolding was quantified using a Varian Eclipse fluorescence spectrophotometer, with a wavelength of 295 nm for excitation and 350 nm for emission, and maintained at 298 K with a temperature-controlled Peltier cell holder (Varian Inc., Palo Alto, CA). The unfolding kinetics exhibited relaxation times that were appropriate for manual mixing techniques. The data

collection strategy was designed to span approximately two to three half-lives, or $>80\%$ of the expected fluorescence signal change between the fully native and denatured states.

Folding kinetic measurements

Prior to analysis protein samples were dialyzed overnight against 20 mM ADA, 100 mM NaCl, 2 mM DTT (pH 6.60) containing either 2.5 M or 3.0 M GuHCl. Under these conditions the protein is essentially completely denatured.[13] Initial studies indicated that the relaxation times for the folding process were more appropriate for stopped-flow data collection. All folding kinetic data was collected using a Kintek SF2000 stopped-flow system (Kintek Corp., Austin, TX). Folding was initiated by a 1:10 dilution of 40 μM denatured protein into 20 mM ADA, 100 mM NaCl (pH 6.60) with denaturant concentrations varying from 0.25 M GuHCl, in increments of 0.05 M, to the midpoint of denaturation as determined by the above described isothermal equilibrium denaturation measurements. The data collection strategy was designed to span approximately five half-lives, or $>97\%$ of the expected fluorescence signal change between the fully denatured and native states.

Kinetic analysis

Both folding and unfolding kinetic data was collected in triplicate at each denaturant concentration, with typically six runs per sample and all data being averaged. The kinetic rate constants and amplitudes, as a function of denaturant concentration, were determined from the time-dependent change in fluorescence intensity implementing a single exponential model:

$$I(t) = A \exp(-kt) + C \quad (2)$$

where $I(t)$ is the intensity of fluorescent signal at time t, A is the corresponding amplitude, k is the observed rate constant for the reaction and C is a constant corresponding to the asymptotic signal limit. If the residuals from the single exponential fit exhibited systematic deviations greater than expected instrument error, a fit to a bi-exponential model was evaluated:

$$I(t) = A_1 \exp(-k_1 t) + A_2 \exp(-k_2 t) + C \quad (3)$$

Folding and unfolding rate constant data were fit to a global function describing the contribution of both rate constants to the observed kinetics as a function of denaturant (chevron plot) as described by Fersht:[40]

$$\ln(k_{obs}) = \ln(k_{f0} \exp(m_{kf}D) + k_{u0} \exp(m_{ku}D)) \quad (4)$$

where k_{f0} and k_{u0} are the folding and unfolding rate constants, respectively, extrapolated to 0 M denaturant, m_{kf} and m_{ku} are the slopes of the linear functions relating $\ln(k_f)$ and $\ln(k_u)$, respectively, to denaturant concentration, and D is denaturant concentration. φ value analysis followed the procedure of Fersht and co-workers:[29]

$$\Delta\Delta G_{\ddagger\text{-}F} = -RT \ln(k_{u\ w.t}/k_{u\ mut}) \quad (5)$$

and

$$\phi_{unf} = \Delta\Delta G_{\ddagger\text{-}F}/\Delta\Delta G_{U-F} \quad (6)$$

where $\Delta\Delta G_{U-F}$ is determined from the isothermal equilibrium data (using the above described method of Pace).

References

1. Nicholson, H., Soderlind, E., Tronrud, D. E. & Matthews, B. W. (1989). Contributions of left-handed helical residues to the structure and stability of bacteriophage T4 lysozyme. *J. Mol. Biol.* **210**, 181–193.
2. Kimura, S., Kanaya, S. & Nakamura, H. (1992). Thermostabilization of *Escherichia coli* ribonuclease HI by replacing left-handed helical Lys95 with gly or asn. *J. Biol. Chem.* **267**, 22014–22017.
3. Stites, W. E., Meeker, A. K. & Shortle, D. (1994). Evidence for strained interactions between side-chains and the polypeptide backbone. *J. Mol. Biol.* **235**, 27–32.
4. Gu, H., Kim, D. & Baker, D. (1997). Contrasting roles for symmetrically disposed β-turns in the folding of a small protein. *J. Mol. Biol.* **274**, 588–596.
5. Kim, K. & Frieden, C. (1998). Turn scanning by site-directed mutagenesis: application to the protein folding problem using the intestinal fatty acid binding protein. *Protein Sci.* **7**, 1821–1828.
6. Masumoto, K., Ueda, T., Motoshima, H. & Imoto, T. (2000). Relationship between local structure and stability in hen egg white lysozyme mutant with alanine substituted for glycine. *Protein Eng.* **13**, 691–695.
7. Takano, K., Yamagata, Y. & Yutani, K. (2001). Role of amino acid residues in left-handed helical conformation for the conformational stability of a protein. *Proteins: Struct. Funct. Genet.* **45**, 274–280.
8. Sibanda, B. L., Blundell, T. L. & Thornton, J. M. (1989). Conformation of β-hairpins in protein structures. A systematic classification with applications to modelling by homology, electron density fitting and protein engineering. *J. Mol. Biol.* **206**, 759–777.
9. Richardson, J. S. (1981). The anatomy and taxonomy of protein structure. *Advan. Protein Chem.* **34**, 167–339.
10. O'Neill, J. W., Kim, D. E., Johnsen, K., Baker, D. & Zhang, K. Y. J. (2001). Single-site mutations induce 3D domain swapping in the B1 domain of Protein L from *Peptostreptococcus magnus*. *Structure*, **9**, 1017–1027.
11. Takano, K., Yamagata, Y. & Yutani, K. (2001). Role of non-glycine residues in left-handed helical conformation for the conformational stability of human lysozyme. *Proteins: Struct. Funct. Genet.* **44**, 233–243.
12. Blaber, M., DiSalvo, J. & Thomas, K. A. (1996). X-ray crystal structure of human acidic fibroblast growth factor. *Biochemistry*, **35**, 2086–2094.
13. Blaber, S. I., Culajay, J. F., Khurana, A. & Blaber, M. (1999). Reversible thermal denaturation of human FGF-1 induced by low concentrations of guanidine hydrochloride. *Biophys. J.* **77**, 470–477.
14. Johnson, D. E., Lu, J., Chen, H., Werner, S. & Williams, L. T. (1991). The human fibroblast growth factor receptor genes: a common structural

arrangement underlies the mechanisms for generating receptor forms that differ in their third immunoglobulin domain. *Mol. Cell. Biol.* **11**, 4627–4634.

15. Johnson, C. M., Cooper, A. & Stockley, P. G. (1992). Differential scanning calorimetry of thermal unfolding of the methionine repressor protein (MetJ) from *Escherichia coli*. *Biochemistry*, **31**, 9717–9724.

16. Orengo, C. A., Jones, D. T. & Thornton, J. M. (1994). Protein superfamilies and domain superfolds. *Nature*, **372**, 631–634.

17. Murzin, A. G., Lesk, A. M. & Chothia, C. (1992). β-Trefoil fold. Patterns of structure and sequence in the kunitz inhibitors interleukins-1β and 1α and fibroblast growth factors. *J. Mol. Biol.* **223**, 531–543.

18. Baird, A., Schubert, D., Ling, N. & Guillemin, R. (1988). Receptor- and heparin-binding domains of basic fibroblast growth factor. *Proc. Natl Acad. Sci. USA*, **85**, 2324–2328.

19. Pantoliano, M. W., Horlick, R. A., Springer, B. A., Van Dyk, D. E., Tobery, T., Wetmore, D. R. *et al.* (1994). Multivalent ligand–receptor binding interactions in the fibroblast growth factor system produce a cooperative growth factor and heparin mechanism for receptor dimerization. *Biochemistry*, **33**, 10229–10248.

20. Springer, B. A., Pantoliano, M. W., Barbera, F. A., Gunyuzlu, P. L., Thompson, L. D., Herblin, W. F. *et al.* (1994). Identification and concerted function of two receptor binding surfaces on basic fibroblast growth factor required for mitogenesis. *J. Biol. Chem.* **269**, 26879–26884.

21. DiGabriele, A. D., Lax, I., Chen, D. I., Svahn, C. M., Jaye, M., Schlessinger, J. & Hendrickson, W. A. (1998). Structure of a heparin-linked biologically active dimer of fibroblast growth factor. *Nature*, **393**, 812–817.

22. Pellegrini, L., Burke, D. F., von Delft, F., Mulloy, B. & Blundell, T. L. (2000). Crystal structure of fibroblast growth factor receptor ectodomain bound to ligand and heparin. *Nature*, **407**, 1029–1034.

23. Stauber, D. J., DiGabriele, A. D. & Hendrickson, W. A. (2000). Structural interactions of fibroblast growth factor receptor with its ligands. *Proc. Natl Acad. Sci. USA*, **97**, 49–54.

24. Estape, D. & Rinas, U. (1999). Folding kinetics of the all-β-sheet protein human basic fibroblast growth factor, a structural homolog of interleukin-1β. *J. Biol. Chem.* **274**, 34083–34088.

25. Varley, P., Gronenborn, A. M., Christensen, H., Wingfield, P. T., Pain, R. H. & Clore, G. M. (1993). Kinetics of folding of the all-β sheet protein Interleukin-1β. *Science*, **260**, 1110–1113.

26. Heidary, D. K. & Jennings, P. A. (2002). Three topologically equivalent core residues affect the transition state ensemble in a protein folding reaction. *J. Mol. Biol.* **316**, 789–798.

27. Liu, C., Gaspar, J. A., Wong, H. J. & Meiering, E. M. (2002). Conserved and nonconserved features of the folding pathway of hisactophilin, a β-trefoil protein. *Protein Sci.* **11**, 669–679.

28. Samuel, D., Kumar, T. K. S., Balamurugan, K., Lin, W.-Y., Chin, D.-H. & Yu, C. (2001). Structural events during the refolding of an all β-sheet protein. *J. Biol. Chem.* **276**, 4134–4141.

29. Fersht, A. R., Matouschek, A. & Serrano, L. (1992). The folding of an enzyme I. Theory of protein engineering analysis of stability and pathway of protein folding. *J. Mol. Biol.* **224**, 771–782.

30. Kim, J., Blaber, S. I. & Blaber, M. (2002). Alternative type I and I′ turn conformations in the β8/β9 β-hairpin of human acidic fibroblast growth factor. *Prot. Sci.* **11**, 459–466.

31. Pace, C. N. & Scholtz, J. M. (1997). Measuring the conformational stability of a protein. In *Protein Structure: A Practical Approach* (Creighton, T. E., ed.), pp. 299–321, Oxford University Press, Oxford.

32. Brych, S. R., Blaber, S. I., Logan, T. M. & Blaber, M. (2001). Structure and stability effects of mutations designed to increase the primary sequence symmetry within the core region of a β-trefoil. *Protein Sci.* **10**, 2587–2599.

33. Srinivasan, N., Anuradha, V. S., Ramakrishnan, C., Sowdhamini, R. & Balaram, P. (1994). Conformational characteristics of asparaginyl residues in proteins. *Int. J. Pept. Protein Res.* **44**, 112–122.

34. Chou, P. Y. & Fasman, G. D. (1974). Prediction of protein conformation. *Biochemistry*, **13**, 222–245.

35. Deane, C. M., Allen, F. H., Taylor, R. & Blundell, T. L. (1999). Carbonyl-carbonyl interactions stabilize the partially allowed Ramachandran conformations of asparagine and aspartic acid. *Protein Eng.* **12**, 1025–1028.

36. Gimenez-Gallego, G., Conn, G., Hatcher, V. B. & Thomas, K. A. (1986). The complete amino acid sequence of human brain-derived acidic fibroblast growth factor. *Biochem. Biophys. Res. Commun.* **128**, 611–617.

37. Linemeyer, D. L., Menke, J. G., Kelly, L. J., Disalvo, J., Soderman, D., Schaeffer, M.-T. *et al.* (1990). Disulfide bonds are neither required, present, nor compatible with full activity of human recombinant acidic fibroblast growth factor. *Growth Factors*, **3**, 287–298.

38. Ortega, S., Schaeffer, M.-T., Soderman, D., DiSalvo, J., Linemeyer, D. L., Gimenez-Gallego, G. & Thomas, K. A. (1991). Conversion of cysteine to serine residues alters the activity, stability, and heparin dependence of acidic fibroblast growth factor. *J. Biol. Chem.* **266**, 5842–5846.

39. Eftink, M. R. (1994). The use of fluorescence methods to monitor unfolding transitions in proteins. *Biophys. J.* **66**, 482–501.

40. Fersht, A. R. (1999). Kinetics of protein folding. *Structure and Mechanism in Protein Science*, W. H. Freeman and Co, New York.

Edited by C. R. Matthews